Bioassembly of Three-Dimensional Embryonic Stem Cell-Scaffold Complexes Using Compressed Gases

Yubing Xie
College of Nanoscale Science and Engineering, University of Albany, Albany, NY, and Nanoscale Science and Engineering Center for Affordable Nanoengineering of Polymeric Biomedical Devices (NSEC-CANPBD), The Ohio State University, Columbus, OH

Yong Yang
Nanoscale Science and Engineering Center for Affordable Nanoengineering of Polymeric Biomedical Devices (NSEC-CANPBD), The Ohio State University, Columbus, OH

Dept. of Chemical and Biomolecular Engineering, The Ohio State University, Columbus, OH 43210

Xihai Kang
Nanoscale Science and Engineering Center for Affordable Nanoengineering of Polymeric Biomedical Devices (NSEC-CANPBD), The Ohio State University, Columbus, OH

Ruth Li
Integrated Biomedical Science Graduate Program, School of Biomedical Science, College of Medicine, The Ohio State University, Columbus, OH

Laboratory of Perinatal Research, Dept. of Obstetrics and Gynecology, The Ohio State University, Columbus, OH

Leonithas I. Volakis
Dept. of Mechanical Engineering, The University of Michigan, Ann Arbor, MI

Xulang Zhang
Nanoscale Science and Engineering Center for Affordable Nanoengineering of Polymeric Biomedical Devices (NSEC-CANPBD), The Ohio State University, Columbus, OH

L. James Lee
Nanoscale Science and Engineering Center for Affordable Nanoengineering of Polymeric Biomedical Devices (NSEC-CANPBD), The Ohio State University, Columbus, OH

Dept. of Chemical and Biomolecular Engineering, The Ohio State University, Columbus, OH 43210

Douglas A. Kniss
Nanoscale Science and Engineering Center for Affordable Nanoengineering of Polymeric Biomedical Devices (NSEC-CANPBD), The Ohio State University, Columbus, OH

Laboratory of Perinatal Research, Dept. of Obstetrics and Gynecology, The Ohio State University, Columbus, OH

Dept. of Biomedical Engineering, The Ohio State University, Columbus, OH

DOI 10.1021/bp.151
Published online March 30, 2009 in Wiley InterScience (www.interscience.wiley.com).

Tissues are composed of multiple cell types in a well-organized three-dimensional (3D) microenvironment. To faithfully mimic the tissue in vivo*, tissue-engineered constructs should have well-defined 3D chemical and spatial control over cell behavior to recapitulate developmental processes in tissue- and organ-specific differentiation and morphogenesis. It is a challenge to build a 3D complex from two-dimensional (2D) patterned structures with the presence of cells. In this study, embryonic stem (ES) cells grown on polymeric scaffolds with well-defined microstructure were constructed into a multilayer cell-scaffold complex using low pressure carbon dioxide (CO_2) and nitrogen (N_2). The mouse ES cells in the assembled constructs were viable, retained the ES cell-specific gene expression of Oct-4, and maintained the formation of embryoid bodies (EBs). In particular, cell viability was increased from 80% to 90% when CO_2 was replaced with N_2. The compressed gas-assisted bioassembly of stem cell-polymer constructs opens up a new avenue for tissue engineering and cell therapy.* © 2009 American Institute of Chemical Engineers *Biotechnol. Prog.,* 25: 535–542, 2009

Additional Supporting Information may be found in the online version of this article.

Current address of Yong Yang: Biomedical Engineering Department, Duke University, Durham, NC.

Current address of Xihai Kang: Atotech USA, Albany, NY.

Correspondence concerning this article should be addressed to L. J. Lee at lee.31@osu.edu or D. A. Kniss at kniss.1@osu.edu.

Keywords: embryonic stem cells, cell-scaffold construct, bioassembly, tissue engineering, compressed gases and 3D

Introduction

Tissue engineering, the in vitro fabrication of three-dimensional (3D) tissue equivalents in a rational and predictable manner, has evolved over the past two decades as a promising solution to the shortage of viable solid organs for transplantation.[1] Using tissue engineering strategies, some tissue constructs have been prepared and have shown promise in initial clinical studies. In addition, a few products such as bioartificial skin and blood vessels have been implemented into clinical practice.[2–5] However, there still lacks efficient and reproducible schemes to assemble neotissues into complex 3D configurations that closely match the architecture of the tissue to be replicated.

Within all biological tissues, the extracellular matrix (ECM) plays an essential role in providing structural support for the cellular elements.[6] In the design and fabrication of tissue-engineered constructs, it is vital to create 3D scaffolds with predefined structure in order to control the spatial organization of cells and to provide cellular, chemical, and physical cues to recapitulate developmental processes in tissue morphogenesis and function.[7,8] Commonly used scaffolds such as fibrous matrices or foams cannot produce well-defined pore structure and cannot localize multiple cell types into specific sites for proper function.[9] Solid free-form fabrication and stereolithography techniques can be used to form well-defined 3D structures,[10,11] but their applications are restricted because of their limited control over the shape and dimensions of the building elements and their rigorous process parameters. Microfabrication technologies have enabled tissue engineers to better understand cell behaviors and guide cell growth in both single and multicellular organisms.[12,13] However, it is limited to two-dimensional, patterned surfaces. It is of paramount importance to assemble these 2D patterned cellular layers into a single 3D construct to mimic the tissue in vivo. For example, the native blood vessel is composed of an outer fibroblastic layer, a medium smooth muscle layer, and an inner endothelial layer. In the process of engineering blood vessel, cell and fiber orientation must be considered. 2D patterned surface can be used to guide the growth of individual layer of cells. However, it is challenge to assemble the 2D patterned surfaces with cells into a 3D structure. Conventional polymer assembly techniques, using either organic solvents or high temperatures, are detrimental to cells[14] and tend to deform the original microstructures.[15] Recently, we have successfully demonstrated that low-pressure carbon dioxide (CO_2) can enhance the interfacial fusion of micro/nanostructures at low temperatures[16,17] and can complete the assembly of polymeric microstructure containing cells at biologically permissive temperature in an aqueous environment with excellent preservation of cell viability and function as well as the original microstructure.[18]

In this article, we further investigated the construction of embryonic stem (ES) cells grown on biodegradable polymeric scaffolds with well-defined architecture into a 3D complex using low pressure gases, including CO_2 and N_2. ES cells have great potential as unlimited cell sources in tissue engineering and cell therapy.[19] In particular, ES cells are excellent platforms for the assembly of in vitro culture systems for the study of stem cell niche and tissue morphogenesis.[20,21] This study highlights the ability to integrate multiple stem cell-scaffold constructs into a tissue complex, by first allowing the individual stem cell types to grow on biodegradable polymeric scaffolds, and then assembling the desired multiple cell-scaffolds into a 3D tissue complex.

Materials and Methods

Preparation of patterned PLGA scaffold

Poly(DL-lactide-*co*-glycolide) (PLGA, Alkermes Medisorb® 5050 DL High IV) was donated by Alkermes (Cincinnati, OH). The CO_2 used was a bone-dry grade supplied by Praxair at a purity of 99.99%. The nitrogen used was also supplied by Praxair at a purity of 99.995%.

Microstructures were patterned and fabricated into PLGA bilayer scaffolds by using photolithography and microembossing methods.[9] Two layers were stacked, orthogonally aligned, and bonded using CO_2.[9] Bonded PLGA scaffolds were cut and fit in a 48-well plate. Scaffolds were sterilized using the UV light in a tissue culture hood.

Cell culture of mouse embryonic stem cells

The mouse CCE ES cell line was a generous gift from StemCell Technologies (Vancouver, Canada).[22,23] Cells were grown on gelatin-coated tissue culture flasks in a maintenance medium consisting of Dulbecco's Modified Eagle's Medium (DMEM with 4.5 g/L D-glucose), supplemented with 15% (v/v) fetal bovine serum (FBS), 100 U/mL penicillin, 100 μg/mL streptomycin, 0.1 mM nonessential amino acids, 10 ng/mL murine recombinant leukemia inhibitory factor (LIF; StemCell Technologies), 0.1 mM monothioglycerol (Sigma Aldrich, St. Louis, MO), 2 mM L-glutamine, and 1 mM sodium pyruvate (Invitrogen, Carlsbad, CA). Cells were passaged every second day before it exceeded 50–70% confluency.

Cell culture on PLGA scaffolds

Scaffolds were coated with 0.02% gelatin (Sigma Aldrich). Mouse ES cells (1×10^5) were seeded on the PLGA scaffolds. After 4 h, scaffolds with cells were transferred to a new 24-well plate and cultured.

Compressed gas-assisted bioassembly

PLGA scaffolds with ES cells were stacked, layer-by-layer, in a sterile container with culture medium under a compressive pressure of 55 kPa and assembled as described elsewhere.[18] Briefly, the container was placed in a pressure vessel (Parr 4660, Parr Instrument Company) and maintained at 37°C through a water jacket. CO_2 was delivered to the vessel and the CO_2 pressure was controlled by an ISCO 500 D high-pressure syringe pump (Teledyne Isco, Lincoln, NE). The CO_2 pressure was increased to ~0.69 MPa at a rate of 0.14 MPa per min, and maintained at 0.69 MPa for 15 min,

followed by a slow pressure release at 0.02 MPa per min. After CO_2 bonding, assembled cell-scaffold constructs were transferred to a 24-well plate and cultured with fresh culture medium. When N_2 was used as the replacement of CO_2, the same compressive pressure (55 kPa) and temperature (37°C) were maintained while the N_2 pressure was increased to ~1.73 MPa at a rate of 0.34 MPa per min, and maintained at 1.73 MPa for 15 min, followed by a slow pressure release at 0.06 MPa per min.

Scanning electron microscopy

The cell-scaffold constructs were fixed with 3% glutaraldehyde in 0.1 M phosphate buffer (pH 7.4) containing 0.1 M sucrose, followed by postfixation in 1% OsO_4 (Sigma Aldrich). After dehydration in serial gradients of ethanol, the samples were dried by infiltration of hexamethyldisilazane (HMDS) using graded HMDS in ethanol (25, 50, 75, 100, 100, and 100%; Ted Pella, Redding, CA). Samples were sputter-coated with gold at an argon pressure of 13.8 kPa for 30 s at a current of 25 mA. This step was repeated twice with 60-s intervals to prevent the samples from overheating. Samples were observed using a Hitachi S-3000H scanning electron microscope (Hitachi High Technologies America, Pleasanton, CA).

Cell stain with CellTracker™ probes

CellTracker™ green CMFDA (5-chloromethylfluorescein diacetate) and orange CMTMR (5-(and-6)-(((4-chloromethyl)benzoyl)amino) tetramethylrhodamine) (Molecular Probes, Eugene, OR) were used to label living ES cells with green and red fluorescence, respectively. After ES cells were trypsinized and harvested, half of the cells were suspended in the CMFDA solution, and the other half in the CMTMR solution (0.5 μM in serum-free medium). They were incubated at 37°C in a CO_2 incubator for 15 min. After washing with phosphate-buffered saline (PBS), 1×10^4 of ES cells stained with CMFDA were seeded into one piece of PLGA scaffold, while 5×10^4 of ES cells stained with CMTMR were seeded into another piece of PLGA scaffold. Scaffolds with cells were placed in cultured medium and cultured overnight. Then, two pieces of PLGA scaffolds were stacked and exposed to CO_2 or N_2 fusion as described earlier. Assembled cell-scaffold constructs were transferred to a 24-well plate and cultured with fresh culture medium for 30 min. After washing with PBS, assembled cell-scaffold constructs were fixed with 3.7% formaldehyde and imaged by a confocal laser scanning biological microscope (FV1000, Olympus America, Melville, NY) with filter sets of 488 and 541 nm.

Cell viability in bioassembled 3D constructs

Constructs were washed with PBS and stained with calcein AM/ethidium homodimer-1 (EthD-1; Molecular Probes) working solution, composed of 4 μM of EthD-1 and 2 μM of calcein AM in PBS, for 30 min at room temperature. Labeled cells were viewed under a laser scanning confocal microscope (510 Meta LSCM, Zeiss, Germany) using the FITC filter, where the green fluorescence indicated live cells labeled by calcein AM. For quantitative analysis of cell viability, cells grown on the cell culture flask were treated with CO_2 and N_2, respectively. Cells were trypsinized and centrifuged. The cells were stained with calcein AM/ethidium homodimer-1 (EthD-1; Molecular Probes) working solution as mentioned earlier. Cells were counted using a hymocytometer under a fluorescence microscope using the FITC/Rhodamine filter. Live cells were revealed in green under FITC filter, and dead cells were revealed in red under Rhodamine filter. Cell viability was calculated as the percentage of green fluorescent cells. The data were presented as the mean ± standard derivation of the mean. A one-way analysis of variance (ANOVA) was performed, and $P < 0.05$ was considered significant. Each experiment was replicated at least twice.

Immunostaining of bioassembled 3D constructs

After fixed with 4% paraformaldehyde/PBS, permeabilized with 0.2% Triton X-100/PBS, and blocked with 5% goat serum in PBS, 3D ES-scaffold constructs were incubated with primary antibodies against Oct-4 (1:50, Santa Cruz Biotechnology, Santa Cruz, CA), which was detected with Alexa Fluor 594 (1:200, Invitrogen). Samples were further stained with 4′-6-diamidino-2-phenylindole (DAPI; 1:200; Sigma Aldrich) at room temperature to reveal the nuclei and observed under the confocal laser scanning biological microscope (FV1000, Olympus).

Protein extraction and immunoblotting

Mouse ESCs grown in tissue culture flasks were treated with low pressure CO_2 and N_2 as described earlier, respectively. Mouse ESCs without any treatment were used as control. These mESCs were lysed for 30 min in ice-cold RIPA lysis buffer [150 mM NaCl, 1% NP-40, 0.5% sodium deoxycholate, 0.1% sodium-dodecyl sulfate (SDS), 50 mM Tris, 2 mM 4-(2-aminoethyl) benzenesulfonyl fluoride hydrochloride (AEBSF), 0.3 μM aprotinin, 130 μM bestatin, 14 μM *N*-(*trans*-epoxysuccinyl)-L-leucine 4-guanidinobutylamide (E-64), 1 mM EDTA, 1 μM leupeptin (Sigma Aldrich), and 1 μg/mL of pepstatin A (USB, Cleveland, Ohio)]. Cell lysates were clarified by centrifugation for 10 min at 12,000 rpm and 4°C, and the supernatants were retained. Aliquots of each sample were assayed for protein concentration using the BCA Protein Assay (Pierce Biotechnology, Rockford, IL) using standards of bovine serum albumin.

Equal amounts of total protein from each lysate (30 μg/lane) were resolved by sodium-dodecyl sulfate polyacrylamide gel electrophoresis and electrophoretically transferred to nitrocellulose. Nonspecific binding was blocked by incubation in Tris-buffered saline (pH 8) containing 0.1% Tween-20 and 5% nonfat dry milk. Membranes were then probed with primary antibodies against β-actin (1:500; Santa Cruz Biotechnology) and Oct-4 (1:200; Santa Cruz Biotechnology) diluted in blocking solution overnight. After washing, the membranes were exposed to horseradish peroxidase-conjugated secondary antibodies and immune complexes were revealed using SuperSignal chemiluminescent substrate (Pierce Biotechnology). Immunoreactive proteins were visualized using the VersaDoc Imaging System (Bio-Rad, Hercules, CA) and analyzed with Quantity One analysis software (Bio-Rad).

RNA extraction and reverse-transcriptase polymerase chain reaction

Mouse ESCs grown in tissue culture flasks were treated with low pressure CO_2 and N_2 as described earlier,

respectively. Mouse ESCs without any treatment were used as control. For total RNA extraction from these cultured mESCs, culture media was aspirated and replaced with TRIzol® reagent (Invitrogen). Total RNA was extracted according to manufacturer's protocol. Following chloroform extraction and centrifugation, the resulting aqueous phase was mixed with an equal volume of 70% ethanol and applied to an RNeasy mini column (QIAGEN, Valencia, CA) and processed according to the manufacturer's protocol.

Total RNA was quantified by spectrophotometric absorbance at 260 nm, and 2 μg from each sample was then reverse-transcribed to cDNA using oligo-dT primers, dNTP mix, 5× first strand buffer, DTT, and SuperScript III RT (all from Invitrogen) with the total RNA samples following manufacturer's protocol. PCR was performed on the reverse transcripts using specific primer pairs sets for mouse *β-actin* (F: 5′-ACAGCTGAGAGGGAAATCGTGCG-3′, R: 5′-ACTTGC GCTCAGGAGGAGCAATG-3′) and *Oct-4* (F: 5′-CGTGGA GACTTTGCAGCCTG-3′, R: 5′-TGGCTGAACACCTTTC CAAAG-3′) at the following cycling conditions: initial denaturing at 94°C for 2 min, followed by 30 cycles of denaturation at 94°C for 30 s, annealing at 55°C for 30 s, and extension at 72°C for 1 min. PCR was performed in a TECHNE TC-312 Thermo Cycler (Techne Incorporated, Burlington, NJ) with Platinum Taq DNA polymerase (Invitrogen) following manufacturer's protocol with a master mix containing appropriate forward and reverse primers along with 10× PCR buffer minus Mg, dNTP, $MgCl_2$, distilled water, and first strand cDNA. PCR products were separated by electrophoresis on a 1% agarose gel containing ethidium bromide, visualized using the VersaDoc Imaging System (Bio-Rad), and analyzed with Quantity One analysis software (Bio-Rad).

Results

Bioassembly of ES cell-scaffold constructs using low pressure CO_2

Mouse ES cells were seeded on the microfabricated PLGA scaffolds, followed by 2 days of maintenance culture. Then two pieces of scaffold with ES cells were stacked layer by layer under a compressive pressure in a sterile container filled with culture medium. After being pressurized at 0.69 MPa CO_2 for 15 min, followed by the slow and constant depressurization at a rate of 0.02 MPa/min, the multiple scaffolds were assembled into a single 3D construct. The assembled 3D construct was transferred to a 24-well plate with fresh ES cell maintenance medium. The SEM image of the assembled 3D ES cell-scaffold construct demonstrated that the ES cells remained attached to the surface or the side wall of the PLGA microstructure after the bioassembly process (Supp. Info. Figure S1).

To better characterize the well-defined layer structure of the assembled 3D ES cell-scaffold constructs, mouse ES cells were labeled with CellTracker™ green CMFDA or orange CMTMR, respectively, and seeded on the microfabricated PLGA scaffolds. After separate overnight culture, the scaffold grown with green CMFDA-labeled ES cells and the scaffold with orange CMTMR-labeled ES cells were assembled following the aforementioned process. The assembled 3D construct was inspected using confocal microscopy. A 3D configuration of the well-defined layered structure is illustrated in Figure 1, with two layers of orange cells at the bottom and two layers of green cells on the top.

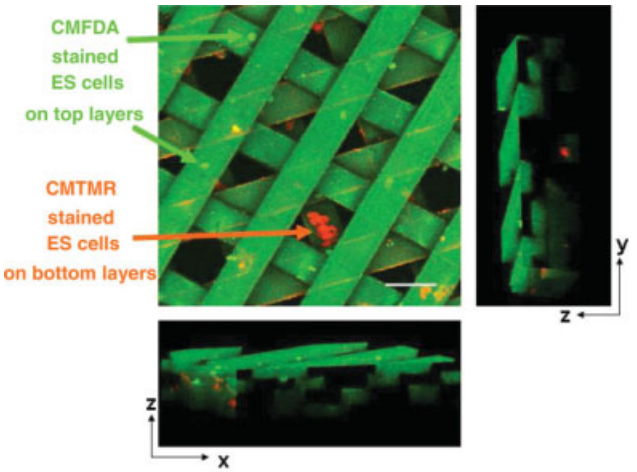

Figure 1. Confocal images of the assembled cell-scaffold construct.

The PLGA microstructure was revealed by autofluorescence in green. The mouse ES cells grown on the top two layers were prelabeled with Cell Tracker™ CMFDA in green, and those on the bottom two layers were prelabeled with Cell Tracker™ CMTMR in orange. Bar = 100 μm.

The images in Figure 1 are the projection of a 3D reconstituted image on the *x-y*, *x-z*, and *y-z* planes.

ES cell survival and Oct-4 retention after CO_2-assisted bioassembly

About 80% of ES cells were viable after CO_2 treatment as detected by LIVE/DEAD staining with calcein AM/EthD-1. All ES cells in the assembled 3D construct expressed nuclear Oct-4 immunoreactivity (Figure 2), which is the canonical marker of pluripotency. This indicated that cells that survived the CO_2-assisted bioassembling process remained undifferentiated and maintained the stem cell phenotype.

Embryoid body formation and maintenance after CO_2-assisted bioassembly

Whether embryoid bodies (EBs) on the bioassembled scaffolds can lead to the differentiation of ES cells in a manner mimicking embryogenesis was examined next. Mouse ES cells were seeded on PLGA 3D scaffolds and grown in medium without LIF to form EBs. After 4 days of cultivation, the PLGA scaffolds containing EBs were stacked layer by layer under a compressive pressure in a sterile container filled with culture medium and experienced CO_2-assisted bioassembly. The confocal microscopy revealed that EBs on the scaffolds were well maintained (Figure 3). Staining in green with calcein AM confirmed that the cells in EBs were viable. Furthermore, the outgrowth of EBs experienced CO_2-assisted bioassembly could differentiate into multiple cell types expressing marker proteins of mesoderm, neuroectoderm, neural cells, cardiac muscle cells, and skeletal muscle cells (Supp. Info. of Ref. 18).

Bioassembly using low pressure N_2

The feasibility of assembling polymeric microstructures containing ES cells with low pressure N_2 was also examined. The procedure was similar to CO_2-assisted bioassembly, except for the pressure level (1.73 vs. 0.69 MPa) and the pressure release rate (0.06 vs. 0.02 MPa per min). The

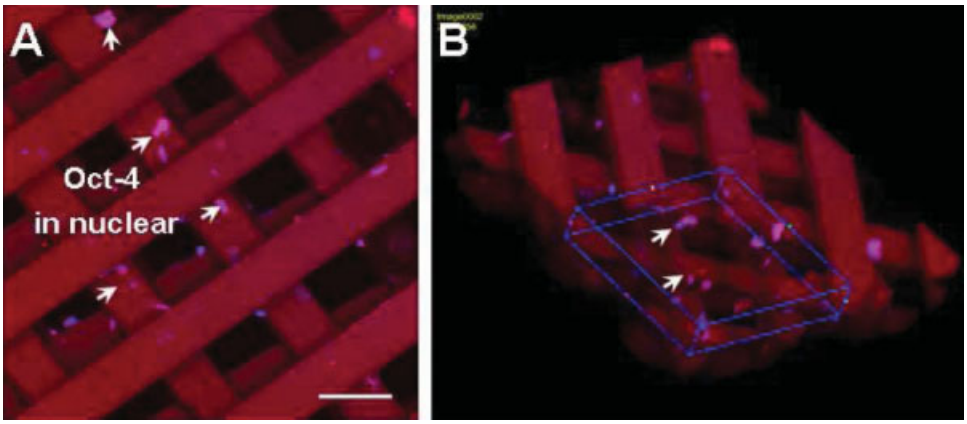

Figure 2. The mouse ES cells grown on PLGA microstructure maintained the expression of Oct-4 after bioassembly (pink: Oct-4; blue: DAPI-stained nuclei).

Bar = 100 μm.

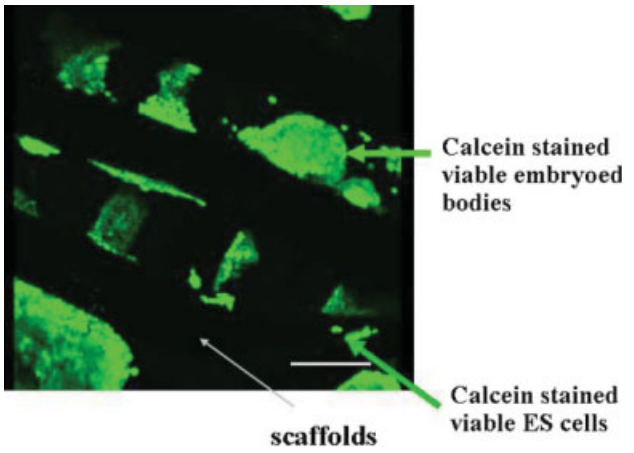

Figure 3. The mouse ES cells formed embryoid bodies and maintained viable after bioassembly.

Bar = 100 μm.

multiple ES cell-scaffold constructs were assembled into a single 3D complex, which was transferred to a fresh ES maintenance medium and cultured as desired. SEM images revealed that ES cells in the 3D complex remained attached after N_2-assisted bioassembly (Figure 4). Labeling with calcein AM in green revealed that cells in the 3D complex were viable (data not shown) after 7 days of culture. Furthermore, immunoblotting and reverse-transcription PCR results (Figures 5a,b, respectively) indicate maintenance of Oct-4 expression after low pressure N_2 exposure, as compared to control. Our previous study revealed that the mouse CCE ESCs which maintained *Oct-4* gene also maintain their differentiation potential after low pressure CO_2 treatment.[18] In our future study, the expression of SSEA-1 and alkaline phosphatase will be further performed to confirm that mESCs maintain their pluripotency after N_2 treatment.

Comparison of N_2 and CO_2 treatment

After N_2 treatment, the pH in the medium remained unchanged. On the contrary, the pH in the medium dropped from 7.4 to 6.5 during CO_2 pressurization (Supp. Info. Table 1). There was no bubble formation in N_2-assisted bioassembly, whereas bubbles were observed after CO_2 depressurization. Compared to low pressure CO_2, N_2-assisted bioassembly improved the cell viability from 80 to 90% as determined on the cells that remain attached (Figure 6). Although the difference in cell viability is not significant, the trend that N_2-assisted bioassembly produced higher cell survival rate than CO_2-assisted bioassembly was repeatable. In particular, a much higher percentage of ES cell attachment after N_2-assisted bioassembly was observed compared to CO_2-assisted bioassembly (100% vs. 60%).

Discussion and Conclusions

The results from this work indicate that CO_2 and N_2 can diffuse into the buffer solution and cultivation media, making surface molecular chains of PLGA mobile, and therefore, fusing polymeric structures. By adjusting the gas pressure, the fusion temperature can be decreased to a biologically permissive temperature. The selection of CO_2 or N_2 pressure was dependent on the type of polymer used. PLGA could be fused at 37°C under either 0.69 MPa CO_2 or 1.73 MPa N_2 pressure in an aqueous environment. Our results demonstrated that low pressure of CO_2 or N_2 had little effect on the behavior of mouse ES cells.

The gas-assisted bioassembly involves three steps: pressurization, CO_2 treatment, and depressurization. Although some mammalian cells can survive a supercritical CO_2 environment for up to 5 min,[24] CO_2 under high pressure could diffuse into the cells reacting with water to produce carbonic acid and altering the pH level within the cell, which could be detrimental to proteins,[25] DNA,[26] and cells.[27] This restricts the applications of supercritical CO_2 in biomedical engineering. Our method only requires low CO_2 pressures to complete interfacial fusion. In our study, the media were buffered by a bicarbonate buffer system. We also tried a much stronger buffer of HEPES (4-(2-hydroxyethyl)-1-piperazineethanesulfonic acid). Although the pH in both medium dropped from 7.4 to 6.5 during pressurization, most of mES cells survived and retained their viability after CO_2 treatment. Extending the CO_2 treatment time from 15 min to 2 h at 1.38 MPa and 37°C did not influence the survival rate of cells (data not shown).

Cells were more sensitive to the depressurization rate than the pressurization rate. When the pressurization time was

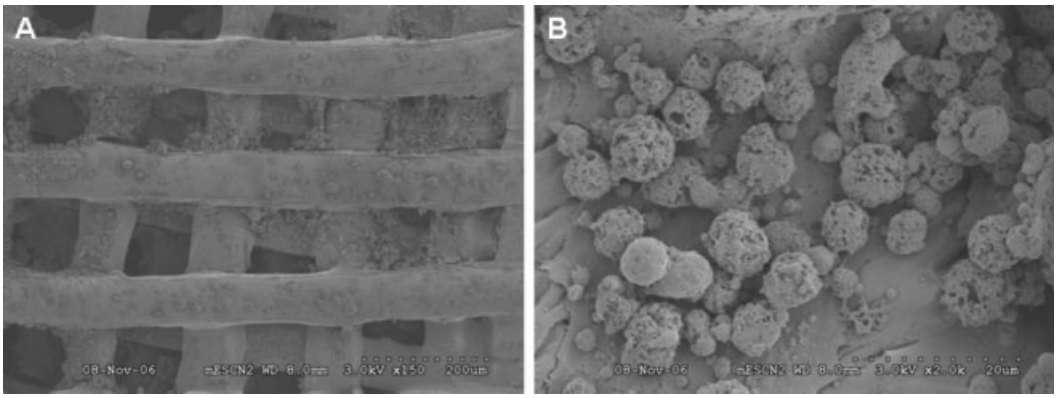

Figure 4. SEM image shows mouse ES cells attachment after N_2-asssited bioassembly.
Bar = 200 μm (A) and 20 μm (B).

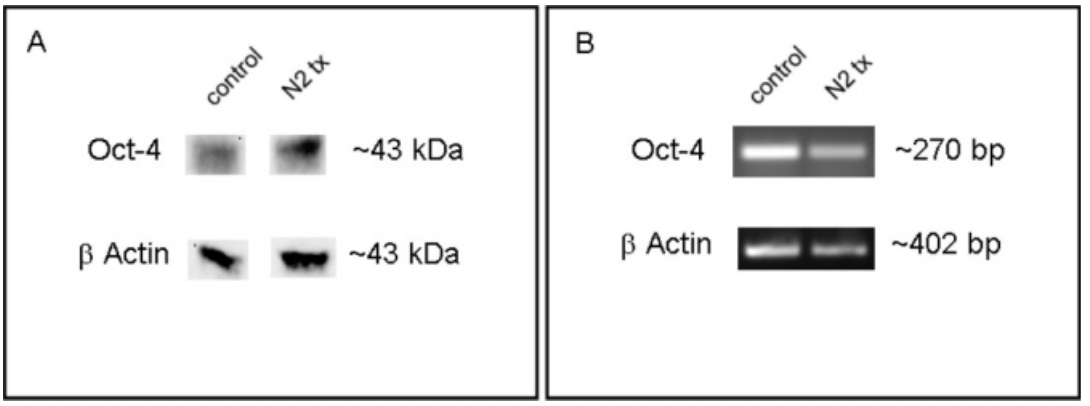

Figure 5. Determination of Oct-4 protein and mRNA expression in mESCs exposed to low pressure N_2 by immunoblotting (A) and reverse-transcription PCR (B), respectively.

varied from 5 to 15 min, no obvious change in cell viability was observed. However, when CO_2 was quickly released (less than 5 min), cell detachment often occurred. By carrying out the depressurization process at a much slower and constant release rate, ES cell survival levels were 80%. Direct observation through a view window during depressurization showed that many bubbles were generated inside the media. These bubbles nucleated and grew around the cells and scaffold, and thus exerted physical stresses on the cells.[28] These stresses and bubble burst near the cell surface resulted in cell detachment in some cases. Formation of bubbles was reduced, even eliminated, when the depressurization process was slowed down.

The mouse ES cells preserved Oct-4 expression after CO_2-treatment, which is one of the most highly enriched genes in early embryogenesis and is expressed in pluripotent ES cells.[29,30] In addition, ES cells formed EBs after CO_2 treatment. The formation of EBs by aggregation of ES cells is one of the critical stages of ES differentiation in vitro, which can lead to differentiation of pluripotent cells in an ordered and predictable manner that shares many features with mouse embryogenesis.[23,31,32] The finding that formed EBs are able to survive the bioassembly process suggests that the method can be used to construct 3D tissue complex by first allowing EBs to differentiate to desired tissue types on biodegradable polymeric scaffolds, and then assemble the desired multiple cell-scaffolds into a 3D construct. For example, ES cells grown on individual scaffolds containing

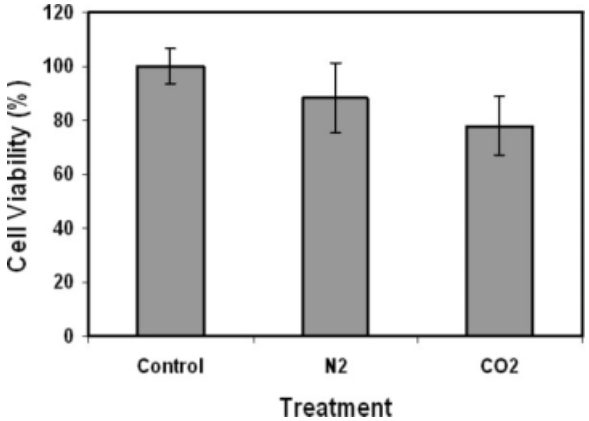

Figure 6. Comparison of N_2-assisted bioassembly with CO_2 on cell viability.

corresponding signal molecules can be simultaneously induced and differentiated into vascular muscle cells[32] and endothelial cells,[33] respectively.

The concern that CO_2 alters the pH of medium, leading to possible adverse affects on cells, promoted us to utilize low pressure N_2 for bioassembly. N_2 is inert, hinders oxidation, has little effect on cells, proteins, and on the metabolic activity within biological substances.[34,35] Low pressure N_2 did not change the pH value in medium, making it more suitable

for bioassembly microstructures containing pH-sensitive cells, proteins, and DNA. The higher percentage of cell attachment and survival rate of ES cells in N_2-asssited bioassembly as determined by LIVE/DEAD staining with calcein AM/EthD-1 may be a result of a lack of pH fluctuation and bubble formation. N_2-asssited bioassembly may provide a more biological benign approach to assemble stem cell-based constructs for tissue engineering and cell therapy.

The low-pressure gases can be used to construct 3D tissue scaffolds for a variety of polymers. The underlying mechanism is that low-pressure gases enhance the polymer chain mobility at the surface far below the glass transition temperature of the polymers.[17] This low-pressure gas-assisted assembly technique is applicable to all polymers that gases can plasticize, in particular, thermoplastic polymers. But the assembly condition will be varied depending on the polymer used. Previously, we demonstrated the assembly of 320 layers of scaffold skeletons using compressed CO_2, each layer having the dimensions of 1 cm $\times$ 1 cm $\times$ 60 μm, into a large scaffold of about 1 cm $\times$ 1 cm $\times$ 2 cm (W $\times$ L $\times$ H).[9] Previously, we have successfully utilized this technique to assemble polymeric scaffolds in gas phase.[9,16,17] In this study, we have demonstrated the capacity to bond polymeric structure in aqueous phase using low-pressure gases. The compressed gases are diffused into water or media. Liquid can facilitate the gas-assisted fusion of polymeric structures so that the bonding force between layers is reduced from 1 MPa (for gas phase bonding) to 0.69 MPa (for aqueous phase bonding) and the bonding time is reduced from 4 h (for gas phase bonding) to 15 min (for aqueous phase bonding). The lower pressure, shorter time, and the presence of water or medium makes it possible to assemble polymeric scaffold in the presence of cells. This low pressure gas-assisted bioassembly has great potential to construct 3D tissue complex of thickness and complicated structures.

Acknowledgments

The authors thank Dr. William Ackerman for his scientific input during the design of the experiments for this manuscript. This material is based upon work supported by the National Science Foundation-sponsored Nanoscale Science and Engineering Center for Affordable Nanoengineering of Polymeric Biomedical Devices (NSEC-CANPBD) at The Ohio State University under award no. EEC-0425626, and by The Ohio State University Perinatal Research Fund.

Literature Cited

1. Langer R, Vacanti JP. Tissue engineering. *Science*. 1993;260: 920–926.
2. L'Heureux N, Paquet S, Labbe R, Germain L, Auger FA. A completely biological tissue-engineered human blood vessel. *FASEB J*. 1998;12:47–56.
3. Marston WA. Dermagraft, a bioengineered human dermal equivalent for the treatment of chronic nonhealing diabetic foot ulcer. *Expert Rev Med Devices*. 2004;1:21–31.
4. Niklason LE, Gao J, Abbott WM, Hirschi KK, Houser S, Marini R, Langer R. Functional arteries grown in vitro. *Science*. 1999;284:489–493.
5. Shin'oka T, Imai Y, Ikada Y. Transplantation of a tissue-engineered pulmonary artery. *N Engl J Med*. 2001;344:532–533.
6. Bell E. Tissue engineering in perspective. In: Lanza RP, Langer RS, Vacanti J, editors. *Principles of Tissue Engineering*, 2nd ed. San Diego: Academic Press; 2000:xxxv-xl.
7. Basu S, Gerchman Y, Collins CH, Arnold FH, Weiss R. A synthetic multicellular system for programmed pattern formation. *Nature*. 2005;434:1130–1134.
8. Lutolf MP, Hubbell JA. Synthetic biomaterials as instructive extracellular microenvironments for morphogenesis in tissue engineering. *Nat Biotechnol*. 2005;23:47–55.
9. Yang Y, Basu S, Tomasko DL, Lee LJ, Yang ST. Fabrication of well-defined PLGA scaffolds using novel microembossing and carbon dioxide bonding. *Biomaterials*. 200;26:2585–2594.
10. Hutmacher DW, Sittinger M, Risbud MV. Scaffold-based tissue engineering: rationale for computer-aided design and solid free-form fabrication systems. *Trends Biotechnol*. 2004; 22:354–362.
11. Sun C, Fang N, Wu DM, Zhang X. Projection micro-stereolithography using digital micro-mirror dynamic mask. *Sens Actuators A Phys*. 2005;121:113–120.
12. Chen CS, Mrksich M, Huang S, Whitesides GM, Ingber DE. Geometric control of cell life and death. *Science*. 1997;276: 1425–1428.
13. Desai TA. Micro- and nanoscale structures for tissue engineering constructs. *Med Eng Phys*. 2000;22:595–606.
14. Shea LD, Smiley E, Bonadio J, Mooney DJ. DNA delivery from polymer matrices for tissue engineering. *Nat Biotechnol*. 1999;17:551–554.
15. King KR, Wang CC, Shin M, Vacanti JP, Borenstein JT. Biodegradable polymer microfluidics for tissue engineering microvasculature. *Mater Res Soc Symp Proc*. 2002;729:3–8.
16. Yang Y, Zeng CC, Lee LJ. Three-dimensional assembly of polymer microstructures at low temperatures. *Adv Mater*. 2004; 16:560–564.
17. Yang Y, Liu DH, Xie YB, Lee LJ, Tomasko DL. Low-temperature fusion of polymeric nanostructures using carbon dioxide. *Adv Mater*. 2007;19:251–254.
18. Yang Y, Xie Y, Kang X, Lee LJ, Kniss DA. Assembly of three-dimensional polymeric constructs containing cells/biomolecules using carbon dioxide. *J Am Chem Soc*. 2006;128:14040–14041.
19. Thomson JA, Itskovitz-Eldor J, Shapiro SS, Waknitz MA, Swiergiel JJ, Marshall VS, Jones JM. Embryonic stem cell lines derived from human blastocysts. *Science*. 1998;282: 1145–1147.
20. Moore KA, Lemischka IR. Stem cells and their niches. *Science*. 2006;311:1880–1885.
21. Vallier L, Pedersen RA. Human embryonic stem cells: an in vitro model to study mechanisms controlling pluripotency in early mammalian development. *Stem Cell Rev*. 2005;1:119–130.
22. Keller G, Kennedy M, Papayannopoulou T, Wiles MV. Hematopoietic commitment during embryonic stem cell differentiation in culture. *Mol Cell Biol*. 1993;13:473–486.
23. Robertson E, Bradley A, Kuehn M, Evans M. Germ-line transmission of genes introduced into cultured pluripotential cells by retroviral vector. *Nature*. 1986;323:445–448.
24. Ginty PJ, Howard D, Rose FR, Whitaker MJ, Barry JJ, Tighe P, Mutch SR, Serhatkulu G, Oreffo RO, Howdle SM, Shakesheff KM. Mammalian cell survival and processing in supercritical CO(2). *Proc Natl Acad Sci USA*. 2006;103:7426–7431.
25. Weder JKP. Influence of supercritical carbon-dioxide on proteins and amino-acids—an overview. *Cafe Cacao* 1990;34:87–96.
26. Tservistas M, Levy MS, Lo-Yim MY, O'Kennedy RD, York P, Humphrey GO, Hoare M. The formation of plasmid DNA loaded pharmaceutical powders using supercritical fluid technology. *Biotechnol Bioeng*. 2001;72:12–18.
27. Dillow AK, Dehghani F, Hrkach JS, Foster NR, Langer R. Bacterial inactivation by using near- and supercritical carbon dioxide. *Proc Natl Acad Sci USA*. 1999;96:10344–10348.
28. Freshney RI. *Culture of Animal Cells: A Manual of Basic Techniques*, 4th ed. New York, NY: Wiley; 2000.
29. Pesce M, Scholer HR. Oct-4: gatekeeper in the beginnings of mammalian development. *Stem Cells*. 2001;19:271–278.
30. Rao RR, Stice SL. Gene expression profiling of embryonic stem cells leads to greater understanding of pluripotency and early developmental events. *Biol Reprod*. 2004;71:1772–1778.

31. Rathjen PD, Lake J, Whyatt LM, Bettess MD, Rathjen J. Properties and uses of embryonic stem cells: prospects for application to human biology and gene therapy. *Reprod Fertil Dev*. 1998;10:31–47.
32. Guan K, Rohwedel J, Wobus AM. Embryonic stem cell differentiation models: cardiogenesis, myogenesis, neurogenesis, epithelial and vascular smooth muscle cell differentiation in vitro. *Cytotechnology*. 1999;30:211–226.
33. Gimond C, Marchetti S, Pagès G. Differentiation of mouse embryonic stem cells into endothelial cells: genetic selection and potential use *in vivo*. In: Turksen K, editor. Embryonic Stem Cell Protocols, Vol. II: Differentiation Models, 2nd ed. Totowa, NJ: Humana; 2006:303–330.
34. Berberich JA, Knutson BL, Strobel HJ, Tarhan S, Nokes SE, Dawson KA. Toxicity effects of compressed and supercritical solvents on thermophilic microbial metabolism. *Biotechnol Bioeng*. 2000;70:491–497.
35. Bothun GD, Knutson BL, Strobel HJ, Nokes SE. Molecular and phase toxicity of compressed and supercritical fluids in biphasic continuous cultures of *Clostridium thermocellum*. *Biotechnol Bioeng*. 2005;89:32–41.

Manuscript received Jun. 26, 2008, and revision received Oct. 26, 2008.